Photophysical and *ab Initio* Studies of Mononuclear Copper(I) Complexes

Jerald A. Simon,[1] William E. Palke, and Peter C. Ford*

Department of Chemistry, University of California, Santa Barbara, California 93106

Received April 4, 1996[⊗]

Described are the photophysical properties of the mononuclear copper(I) complexes CuL_4^+ (L = pyridine (py), 4-methylpyridine, 4-phenylpyridine, or acetonitrile), $Cu(lut)_3^+$ (lut = 2,6-lutidine), and $Cu(lut)_2^+$. Each of these compounds as their solid PF_6^- salts display a relatively long-lived (>1 μs), visible range emission at both ambient temperature and at 77 K but not in fluid solutions. Also reported are the results for *ab initio* calculations at the restricted Hartree−Fock self-consistent field level to probe the natures of lower energy excited states of the hypothetical species CuL_n^+ (L = NH_3, CH_3CN, or py; n = 1−4). These results point to an assignment of the lowest energy, luminactive excited states as being largely metal centered, d → s in character for each of the above complexes with the possible exception of the CuL_4^+ species where L is py or a substituted analogue. In the case of $Cu(py)_4^+$ the *ab initio* calculations indicate a metal-to-ligand charge transfer to be the lowest energy Franck−Condon state, although the similarities of emission band shapes, energies, and lifetimes among the various complexes suggest a common d → s assignment.

Introduction

Described here are photophysical and *ab initio* studies of some mononuclear copper(I) complexes of the type CuL_n^+, where L is a neutral nitrogen donor ligand. Mono- and polynuclear complexes of d^{10} metal centers display remarkably rich luminescence and photophysical properties.[2−18] For example, the luminescence spectrum of the tetranuclear Cu(I) cluster $Cu_4I_4(py)_4$ (**A**, py = pyridine), a copper tetrahedron face capped by iodines with a pyridine at each vertex,[19] displays two emission bands (λ_{max}^{em} = 690 and 490 nm in ambient toluene) with different lifetimes (τ = 10.6 and 0.45 μs, respectively).[2−7] *Ab initio* calculations[20] at the restricted Hartree−Fock self-consistent field (RHF-SCF) level demonstrated the lowest energy Franck−Condon excited state (ES) of **A** to be a roughly equal mix of Cu_4I_4 "d → s" and halide-to-metal charge transfer (XMCT) character with the receptor "s" orbital in fact being a delocalized metal−metal bonding MO. We have termed this a "cluster centered" (CC) excited state.[2] The next ES was calculated to be primarily halide-to-ligand π^* charge transfer (XLCT) in character. Overlap population analyses showed increased Cu−Cu and decreased Cu−I bonding in the "cluster

[⊗] Abstract published in *Advance ACS Abstracts,* October 1, 1996.

(1) Taken in part from the Ph.D. dissertation of J.A.S., University of California, Santa Barbara, 1994.
(2) Ford, P. C.; Vogler, A. *Acct. Chem. Res.* **1993**, *26*, 220−226.
(3) (a) Kyle, K. R.; DiBenedetto, J. A.; Ford, P. C. *J. Chem. Soc., Chem. Commun.* **1989**, 714−715. (b) Kyle, K. R.; Ford, P. C. *J. Am. Chem. Soc.* **1989**, *111*, 5005−5006. (c) Kyle, K. R.; Palke, W. E.; Ford P. C. *Coord. Chem. Rev.* **1990**, *97*, 35−46. (d) Kyle, K. R.; Ryu, C. K.; Ford, P. C. *J. Am. Chem. Soc.* **1991**, *113*, 2954−2965. (e) Døssing, A.; Ryu, C. K.; Kudo, S.; Ford, P. C. *J. Am. Chem. Soc.* **1993**, *115*, 5132−5137. (f) Ford, P. C. *Coord. Chem. Rev.* **1994**, *132*, 129−140. (g) Tran, D.; Ryu, C. K.; Ford, P. C. *Inorg. Chem.* **1994**, *33*, 561−566.
(4) (a) Vogler, A.; Kunkely, H. *J. Am. Chem. Soc.* **1986**, *108*, 7211−7212. (b) Hardt, H. D.; Pierre, A. *Inorg. Chim. Acta* **1977**, *25*, L59−L60 and references cited therein. (c) Eitel, E.; Oelkrug, D.; Hiller, W.; Strähle, J. *Z. Naturforsch.* **1980**, *35b*, 1247−1253. (d) Hardt, H. D.; Stroll, H.-J. *Z. Anorg. Allg. Chem.* **1981**, *480*, 193−198, 199−204.
(5) (a) Ryu, C. K.; Kyle, K. R.; Ford, P. C. *Inorg. Chem.* **1991**, *30*, 3982−3986. (b) Sabin, F.; Ryu, C. K.; Vogler, A.; Ford, P. C. *Inorg. Chem.* **1992**, *31*, 1941−1945. (c) Ryu, C. K.; Vitale, M.; Ford, P. C. *Inorg. Chem.* **1993**, *32*, 869−874.
(6) (a) Rath, N. P.; Holt, E. M.; Tanimura, K. *Inorg. Chem.* **1985**, *24*, 3934. (b) Rath, N. P.; Maxwell, J. L.; Holt, E. M. *J. Chem. Soc., Dalton Trans.* **1986**, 2449. (c) Tompkins, J. A.; Maxwell, J. L.; Holt, E. M. *Inorg. Chim. Acta* **1987**, *127*, 1.
(7) (a) Henary, M.; Zink, J. I. *J. Am. Chem. Soc.* **1989**, *111*, 7404−7411. (b) Henary, M.; Zink, J. I. *Inorg. Chem.* **1991**, *30*, 3111−3112. (c) Lai, D. S.; Zink, J. I. *Inorg. Chem.* **1993**, *32*, 2594−2596.
(8) (a)Yam, V. W. W.; Lee, W. K.; Lai, T. F. *Organometallics* **1993**, *12*, 2383. (b) Yam, V. W. W.; Lee, W. K.; Yeung, P. K. Y.; Phillips, D. *J. Phys. Chem.* **1994**, *98*, 7545. (c) Yam, V. W. W.; Lo, K. W. L.; Chueng, K. K. *Inorg. Chem.* **1995**, *34*, 4013−4014.
(9) (a) Buckner, M. T.; Matthews, T. G.; Lytle, F. E.; McMillin, D. R. *J. Am. Chem. Soc.* **1979**, *101*, 5846−5848. (b) Casadonte, D. J.; McMillin, D. R. *J. Am. Chem. Soc.* **1987**, *109*, 331−337. (c) Crane, D. R.; DiBenedetto, J. A.; Palmer, C. E. A.; McMillin, D. R.; Ford, P. C. *Inorg. Chem.* **1988**, *27*, 3698−3700. (d) Stacy, E. M.; McMillin, D. R. *Inorg. Chem.* **1990**, *29*, 393−396. (e) Crane, D. R.; Ford, P. C. *J. Am. Chem. Soc.*, **1990**, *112*, 6871−6875. (f) Everly, R. M.; Ziessel, R.; Suffert, J. McMillin, D. R. *Inorg. Chem.* **1991**, *30*, 559−561. (g) Everly, R. M.; McMillin, D. R. *J. Phys. Chem.* **1991**, *95*, 9071−9075.
(10) (a) Shinozaki, K.; Kaizu, Y. *Bull. Chem. Soc. Jpn.* **1994**, *67*, 2435−2439. (b) Catellano, F. N.; Ruthkosky, M.; Meyer, G. J. *Inorg. Chem.* **1995**, *34*, 3−4.
(11) Horvath, O.; Fendler, J. H.; Stevenson, K. L. *Inorg. Chem.* **1993**, *32*, 227−230.
(12) Stevenson, K. L.; Knorr, D. W.; Horvath, A. *Inorg. Chem.* **1996**, *35*, 835−839.
(13) Kutal, C. *Coord. Chem. Rev.* **1990**, *99*, 213−252.
(14) (a) Parker, W. L.; Crosby, G. A. *J. Phys. Chem.* **1989**, *93*, 5692−5696. (b) Assefa, Z.; Destefano, F.; Gerepapaghi, M. A.; LaCasce, J. H., Jr.; Ouellete, S.; Corson, M. R.; Nagle, J. K.; Patterson, H. *Inorg. Chem.* **1991**, *30*, 2862.
(15) (a) Li, D.; Che, C. M.; Peng, S. M.; Liu, S. T.; Zhou, Z. Y.; Mak, T. C. W. *J. Chem. Soc., Dalton Trans.* **1993**, 189. (b) Hong, X.; Cheung, K. K.; Guo, C.-X.; Che, C. M. *J. Chem. Soc., Dalton Trans.* **1994**, 1867.
(16) (a) Harvey, P. D.; Gray, H. B. *J. Am. Chem. Soc.* **1988**, *110*, 2145−2147. (b) McCleskey, T. M.; Gray, H. B. *Inorg. Chem.* **1992**, *31*, 1733−1734. (c) Hubig, S. M.; Drouin, M.; Michel, A.; Harvey, P. D. *Inorg. Chem.* **1992**, *31*, 3688.
(17) (a) Balch, A. L.; Nagle, J. K.; Oram, D. E.; Reedy, P. E., Jr. *J. Am. Chem. Soc.* **1988**, *110*, 454−462. (b) Balch, A. L.; Catalano, V. J.; Olmstead, M. M. *J. Am. Chem. Soc.* **1990**, *112*, 2010−2011. (c) Larson, L. J.; McCauley, E. M.; Weisshurt, B.; Tinto, D. C. *J. Phys. Chem.* **1995**, *99*, 7218−7126.
(18) (a) Wang, S.; Fackler, J. P., Jr.; King, C.; Wang, J. C. *J. Am. Chem. Soc.* **1988**, *110*, 3308. (b) King, C.; Khan, M. N. I.; Staples, R. J.; Fackler, J. P., Jr. *Inorg. Chem.* **1992**, *31*, 3626. (c) Asssefa, Z.; McBurnett, B. G.; Staples, R. J.; Fackler, J. P., Jr. *Inorg. Chem.* **1995**, *34*, 4965−4972, and references cited therein.
(19) Raston, C. L.; White, A. H. *J. Chem. Soc., Dalton Trans.* **1976**, 2153−2156.
(20) (a) Vitale, M.; Palke, W. E.; Ford, P. C. *J. Phys. Chem.* **1992**, *96*, 8329−8336. (b) Vitale, M.; Ryu, C. K.; Palke, W. E.; Ford, P. C. *Inorg. Chem.* **1994**, *33*, 561−566.

S0020-1669(96)00367-9 CCC: $12.00

centered" state relative to the ground state (GS),[20] while the XLCT state displayed little change in Cu−Cu or Cu−I bonding but a moderate increase in the Cu−N bond order. Thus, the weak coupling between these ES results from the different orbital parentages, leading to distortions along independent coordinates.

Emissive metal-to-ligand charge transfer (MLCT) states dominate the photophysics of mononuclear Cu(I) complexes with chelating ligands such as 2,9-dimethyl-1,10-phenanthroline (dmp) and 2,9-diphenyl-1,10-phenanthroline (dpp).[9,10] For example, $Cu(dmp)_2^+$ displays MLCT absorption at $\lambda_{max}^{abs} = 454$ nm and emission at $\lambda_{max}^{em} = 670$ nm ($\tau_{em} = 90$ ns) in 298 K CH_2Cl_2. Bulky substituents adjacent to the coordination site are necessary for luminactive behavior; the bis(1,10-phenanthroline) complex $Cu(phen)_2^+$ is not emissive under comparable conditions. Emission lifetimes and quantum yields for $Cu(dmp)_2^+$ and $Cu(dpp)_2^+$ in CH_2Cl_2 are quenched by nucleophilic anions and by more basic solvents,[9] and these data were interpreted in terms of an exciplex quenching mechanism where the (formally) d^9 copper in the MLCT state is susceptible to reaction with nucleophiles. Independent of the "exciplex" mechanism, generation of the "d^9" metal center of the MLCT state should lead to Jahn−Teller distortion of the d^{10} Cu(I) complex over radial and angular coordinates.[10a] This may bring the ES and GS surfaces closer and result in enhanced nonradiative deactivation rates. Strategically located bulky substituents inhibit such distortion.[9f]

Emission from Cu(I) → diimine ligand charge transfer states has also been observed from mononuclear complexes with the bulky ligand triphenylphosphine, e.g., the absorption and emission spectra of $Cu(PPh_3)_2(phen)^+$ give $\lambda_{max}^{abs} = 365$ nm (in 298 K ethanol) and $\lambda_{max}^{em} = 600$ nm (in 77 K ethanol), respectively.[9a,b] A long-lived, structured phosphorescence deriving from a phenanthroline localized triplet $\pi\pi^*$ state was also observable. Apparently, the intraligand and MLCT states have sufficiently different geometries as a result of their respective d^{10} and d^9 electronic configurations; the energy barrier between them inhibits equilibration at low *T*.

Although Cu(I) in ammoniated aqueous solution forms di- and triammine species that produce H_2 upon UV irradiation, no luminescence has been detected for these species.[11] However, luminescence attributed to trihalo complexes has been observed upon UV irradiation of aqueous Cu(I) at high halide salt concentrations (1−5 M).[12] The emission wavelength varies little with the halide, 475 nm for Cl^-, 465 nm for Br^-, and 493 nm for I^-, but emission lifetimes are halide dependent.

Clearly, copper(I) complexes display a wide variety of excited states and remarkably rich photophysical and photochemical properties. The phenomenological observations indicate dramatic sensitivity to complex nuclearity, to ligand steric and electronic effects, to the medium, etc. The present experimental and *ab initio* computational investigation of the mononuclear complexes was initiated with the goal of gaining better insight into the relationships between structure and photophysical properties of such d^{10} species.

Experimental Section

Syntheses. Tetrakis(acetonitrile)copper(I) hexafluorophosphate, $[Cu(acn)_4]PF_6$ (**I**) was prepared by the method of Kubas.[21]

The tetrakis(pyridine) analogues $[Cu(py)_4]PF_6$ (**II**)[22,23] and $[Cu(py\text{-}d_5)_4]PF_6$ were prepared as follows. A portion of $[Cu(acn)_4]PF_6$, typically about 100 mg, was placed in a Schlenk tube, which was sealed with a rubber septum and then evacuated and back-filled with argon or nitrogen. A 3 mL volume of reagent pyridine (or pyridine-d_5) that had been degassed by three freeze−pump−thaw cycles was transferred to the Schlenk tube by a cannula, and the resulting solution was allowed to stir for 2 min, after which degassed diethyl ether (20 mL) was added to precipitate the product. The yellow product was washed twice with 20 mL portions of diethyl ether, vacuum dried, and then stored under an argon atmosphere. Elemental analysis (Desert Analytics) showed good agreement between theoretical and experimental values of the percentage compositions for carbon, hydrogen, and nitrogen. Found (theoretical value): C, 45.76 (45.76)%; H, 3.89 (3.84)%; N, 10.48 (10.67)%.

Bis(2,6-lutidine)copper(I) hexafluorophosphate, $[Cu(lut)_2]PF_6$ (**IV**),[24] was prepared by adding the $[Cu(acn)_4][PF_6]$ to a solution of lutidine (vacuum distilled prior to use) in hot ethanol at a slight stoichiometric excess. Boiling ethanol was added until a limpid solution was achieved. The flask was sealed with a septum, evacuated and refilled with argon three times, and placed in the freezer overnight. Needlelike colorless crystals formed and were recovered and stored under argon until needed. Elemental analysis showed reasonable agreement between theoretical and experimental values. Found (theoretical value): C, 38.52 (39.76)%; H, 4.07 (4.29)%; N, 6.78 (6.63)%.

Tris(2,6-lutidine)copper(I) hexafluorophosphate, $[Cu(lut)_3]PF_6$ (**III**),[25] was prepared by adding excess lutidine to $[Cu(acn)_4][PF_6]$ under argon in a Schlenk tube. The product was precipitated by the addition of diethyl ether. The white product was then washed with two portions of diethyl ether. Elemental analysis showed good agreement between theoretical and experimental values for carbon, hydrogen, and nitrogen: Found (theoretical value): C, 47.56 (47.59)%; H, 5.09 (5.13)%; N, 7.89 (7.92)%.

Tetrakis(4-picoline)copper(I) hexafluorophosphate, $[Cu(pic)_4]PF_6$ (**V**),[26] was prepared by dissolving $[Cu(acn)_4][PF_6]$ in redistilled 4-picoline under argon and then adding diethyl ether to form a precipitate, which was separated by filtration. Proportions of all reactants used were the same as for the synthesis of **II**.

Tetrakis(4-phenylpyridine)copper(I) hexafluorophosphate, $[Cu(phpy)_4]PF_6$ (**VI**), was prepared by dissolving the ligand in acetone and degassing by two freeze−pump−thaw cycles. This solution was transferred via cannula to a Schlenk tube containing a stoichiometric amount of $[Cu(acn)_4]PF_6$ under argon. After a few minutes of stirring, all solids dissolved. The resulting solution was frozen by immersing the tube in liquid nitrogen (LN_2) and then allowing it to thaw slowly under vacuum. After the acetone was removed, a yellow oil coated the inside of the Schlenk tube, which was transferred to the glovebox. The oil turned into a powder after vigorous scraping with a spatula.

Spectroscopic Methods. Absorption spectra were recorded using an Olis modified Cary 118 spectrophotometer and corrected by subtracting solvent backgrounds. Solutions were prepared by loading the sample (a few milligrams) into a weighed volumetric flask in an argon filled glovebox, reweighing, adding degassed solvent to volume, and transferring via cannula to a deaerated 1.0 cm path length quartz absorbance cell.

Emission and excitation spectra were collected on a SPEX Fluorolog II spectrofluorimeter. Solid and liquid samples were loaded into quartz tubes under anaerobic conditions and corrected for background spectra of the appropriate solvent or, for solids, of $MgCO_3$. For variable temperature measurements, an Oxford Instruments Cryostat was used in the sample compartment of the spectrofluorimeter. A quartz dewar flask filled with LN_2 was used for samples at 77 K. A correction file for excitation spectra was generated by using the ratio of the absorbance and excitation spectra of a 1.0 mM $[Ru(bpy)_3]Cl_2$ solution in ethanol.

The SPEX Fluorolog was used to measure solid state emission quantum yields using the method of Wrighton et al.[27] A 1.0 × 0.2 cm rectangular cell was filled with the sample and scanned through the

(21) Kubas, G. *Inorg. Synth.* **1990**, *28*, 68−70.
(22) Nilsson, K.; Oskarsson, A. *Acta Chem. Scand. A* **1982**, *36*, 605−610.
(23) Chen, K.; Iwamoto, R. *Inorg. Nucl. Chem. Lett.* **1968**, *4*, 499−502.
(24) Habiyakare, A.; Lucken, E.; Bernardinelli, G. *J. Chem. Soc., Dalton Trans.* **1991**, 2269−2273.
(25) Habiyakare, A.; Lucken, E.; Bernardinelli, G. *J. Chem. Soc., Dalton Trans.* **1992**, 2591−2599.
(26) Lewin, A.; Cohen, I.; Michl. R. *Inorg. Nucl. Chem. Lett.* **1974**, *36*, 1951−1957.
(27) Wrighton, M. S.; Ginley, D. S.; Morse, D. L. *J. Phys. Chem.* **1974**, *78*, 2229−2233.

excitation and emission wavelengths. The same cell was then filled with $MgCO_3$ and scanned through the excitation wavelength. The quantum yield was then calculated as the integrated emission of the sample divided by the difference between the reflected excitation light from the $MgCO_3$ blank minus that reflected from the sample. It was found necessary to detune the fluorimeter so the photomultiplier tube (PMT) signal did not saturate while the light reflected from the $MgCO_3$ blank was measured.

Emission lifetimes were measured using the third harmonic of a Continuum NY60 Nd/YAG laser (355 nm, pulse width ~10 ns) as an excitation source. The emission decay was followed by using an RCA 8852 PMT mounted on a SPEX single monochromator set at λ_{max}^{em} that fed into a Tektronix 7912AD programmable digitizer. The data were analyzed using an exponential fitting routine (ASYST software) run on an IBM compatible 486 computer.

Emission spectra of $[Cu(acn)_4]PF_6$ were recorded by exciting the solid sample with the fourth harmonic (266 nm) of the Continuum NY60 YAG laser. The emission was detected by using a Princeton Instruments LN-CCD detector mounted on an Acton Research SpectraPro-275 triple grating spectrograph.

Infrared spectra were recorded on a Bio-Rad FTS-60 Fourier transform spectrometer. Spectra of neat liquids were collected in NaCl cells. Spectra of copper complexes were recorded as solids in KBr disks except for $[Cu(acn)_4]PF_6$, which formed a colored product when pressed into a KBr disk. A sample of the latter was instead prepared by evaporating a concentrated solution of the complex in acetonitrile on a NaCl disk using a stream of argon. Spectra were produced from 64 scans with a 2 cm^{-1} resolution and a 1 cm^{-1} aperture.

Reflectance spectra were collected against magnesium carbonate on an Olis modified Cary-14 equipped with a collecting sphere. A $MgCO_3$ versus $MgCO_3$ background was subtracted from the collected spectra to allow for differences in the optical path. The spectra were processed using the Kubelka−Monk technique.[28] This was not effective for complexes which undergo room temperature emission since there is no monochromator between the sample and the photodetector to differentiate between reflected and emitted light.

Computational Methods. *Ab initio* calculations were run on VAX 3100 and 3540 computers using the COLUMBUS set of programs.[29] These programs make efficient use of symmetry to lessen the computer power required to carry out the necessary computations. Restricted Hartree−Fock wave functions, which give pure spin states, were used, and the total energy was calculated in terms of shell averaged Coulomb and exchange integrals. This allowed for calculation of all closed shell states and many open shell cases. The calculations did not optimize structural parameters, so excited state calculations were largely based on known or estimated ground state structures; *i.e.*, the ES calculated are Franck−Condon states formed by vertical electronic excitation, and nuclear rearrangement was only considered in limited cases. Basis sets and other computational details are the same as those used in previous studies.[20,30]

The geometries used were derived from X-ray structural data and adapted for the imposed symmetry, preserving bond lengths while tweaking angles and giving reasonable estimates for the hydrogen atom positions or were estimated from molecular modeling calculations. In some cases, one-dimensional potential surfaces were generated by changing a metal−ligand bond distance or bond angle.

Results and Discussions

Absorption Spectra. The electronic absorption spectra of the copper(I) complexes studied are dominated by metal-to-ligand charge transfer (MLCT) and intraligand (IL) bands with large extinction coefficients in the UV or near UV. Absorption spectra recorded in ambient temperature solutions are summarized in Table 1.

Table 1. Absorption Spectra of Mononuclear Cu(I) Complexes in Solution

complex	solvent	λ (nm)	ϵ (10^3 M^{-1} cm^{-1})
$[Cu(acn)_4][PF_6]$ (**I**)	acetonitrile	210	22.2
		227 sh	10.6
$[Cu(lut)_2][PF_6]$ (**III**)	lutidine	315 sh	6.4
$[Cu(lut)_3][PF_6]$ (**IV**)	lutidine	315 sh	6.8
$[Cu(py)_4][PF_6]$ (**II**)	pyridine	330	6.9
$[Cu(pic)_4][PF_6]$ (**V**)	4-picoline	329	8.5
$[Cu(bpy)_2][PF_6]$	4/1 EtOH/MeOH	437	4.4
		521 sh	1.46
$[Cu(phen)_2][PF_6]$	4/1 EtOH/MeOH	438	4.8
		521 sh	1.21

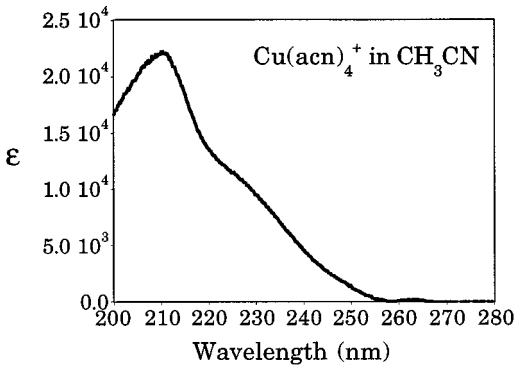

Figure 1. Spectrum of $[Cu(acn)_4]PF_6$ in acetonitrile solution.

Solid $[Cu(acn)_4]PF_6$ is colorless and forms an air stable, colorless solution in acetonitrile (Figure 1). The observable bands appear at 210 (λ_{max}) and 230 nm (shoulder) with large extinction coefficients and tail off to ~260 nm. The free acetonitrile π to π^* and n to π^* transitions occur at much higher energy.[31] A precedent for a MLCT assignment for the UV absorption band of an acetonitrile complex is the ruthenium(II) species $Ru(NH_3)_5(acn)^{2+}$, which displays a MLCT band at 226 nm.[32] The IR spectrum of **I** in KBr displays the pair of bands (2340 m and 2359 m cm^{-1}) in the triple bond region characteristic of acetonitrile and its complexes. The two bands are the ν_{CN} plus a combination band due to coupling of the symmetric CH_3 deformation and the C−C stretch. For **I**, both are shifted to higher frequency (relative to free ligand) as is typical when acn is bound to a Lewis acid with little d → π_L^* back-bonding.[32]

Solutions of $[Cu(py)_4]PF_6$ and $[Cu(pic)_4]PF_6$ in the respective free ligands as solvents show strong bands at 330 and 329 nm which have been assigned to MLCT transitions.[33] These appear at substantially lower energy than free ligand $\pi_L\pi_L^*$ transitions and the MLCT bands of **I**. However, the methyl substituent of 4-picoline has minimal effect on the MLCT λ_{max}. Attempts to record spectra of CuL_4^+ ions in solvents other than the free ligands L resulted in large losses in MLCT band intensities, presumably the result of ligand dissociation from the labile $3d^{10}$ copper centers. This behavior effectively limited the complexes for which room temperature solution absorbance could be measured. The less labile complexes of the bidentate ligands bpy and phen allowed acquisition of spectra in other solvents.

The salts of the bis and tris lutidine complexes **III** and **IV** gave identical electronic spectra when dissolved in lutidine (2,6-dimethylpyridine) because the Cu(I) lability leads to equilibrium

(28) Wendlandt, W. W.; Hecht, H. G. *Reflectance Spectroscopy*; Interscience Publishers: New York, 1966; pp 46−90.
(29) Shephard, R.; Shavitt, I.; Pitzer, R. M.; Comeau, D. C.; Pepper, M.; Lishka, H.; Szalay, P. G.; Ahlrichs, R.; Brown, F. B.; Zhao, J. G. *Int. J. Quantum Chem., Quantum Chem. Symp.* **1988**, *22*, 149−165.
(30) Vitale, M. Ph.D. Thesis, University of California, Santa Barbara, 1992.
(31) Calvert, J. G.; Pitts, J. N. *Photochemistry*; John Wiley & Sons: New York, 1966; p 455.
(32) Clarke, R. E.; Ford, P. C. *Inorg. Chem.* **1970**, *9*, 227.
(33) Kitagawa, S.; Munakata, M.; Higashie, A. *Inorg. Chim. Acta* **1992**, *59*, 219−223.

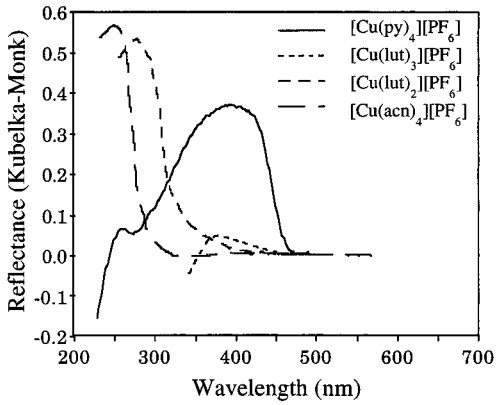

Figure 2. Diffuse reflectance of emissive copper(I) solids.

mixtures of metal centered chromophores, presumably dominated by $Cu(lut)_3^+$. The single band at a wavelength longer than the solvent cutoff (~280 nm) is a shoulder at 315 nm. The spectrum of $lutH^+$ in 4/1 (v/v) EtOH/MeOH solution showed no absorbance below 300 nm, so it is unlikely that this is an intraligand $\pi_L\pi_L^*$ band. A MLCT assignment is suggested in this case as well. The blue shift relative to **II** may be due to the lower coordination number of the Cu(I) owing to the steric bulk of the *o*-methyls. The result would be a lower electron density at the metal center raising the energy required for charge transfer from the metal. Methyl substitution should also shift the MLCT band to the blue;[34] however, this effect proved to be relatively minor for the 4-picoline complex **V**.

For comparison, the absorption spectra of bis(diimine) complexes, $[Cu(phen)_2]PF_6$ and $[Cu(bpy)_2]PF_6$ are dominated by visible range MLCT bands owing to the low energies of the delocalized π-antibonding orbitals of diimine ligands. This is consistent with free ligand reduction potentials, which are much less negative for bpy and phen ($E_{1/2} = -2.11$ and -2.17 V vs SCE in dimethylformamide (DMF), respectively) than for free py (-2.66 V) under the same conditions.[35]

Diffuse Reflectance Spectra. Each of the solid samples showed an absorption edge at a significantly longer wavelength than the absorption band(s) observed in the solution spectra. For example, the onset of absorption in the reflectance spectrum of $[Cu(py)_4]PF_6$ occurs at ~460 nm, about 8×10^3 cm^{-1} lower in energy than the MLCT maximum observed in pyridine solution (Figure 2). Similarly the onset of absorption in reflectance spectra of the solids $[Cu(acn)_4]PF_6$ (~300 nm), $[Cu(lut)_2]PF_6$ (~390 nm), $[Cu(lut)_3]PF_6$ (~430 nm), and $[Cu(bpy)_2]PF_6$ (~700 nm) were considerably to the red of maxima recorded in the solution phase spectra. Presumably, the band edge absorptions seen in the reflectance spectra represent spin forbidden transitions too weak to be evident in dilute solutions which are prominent in the solids owing to the high effective concentrations.

Luminescence Properties. The photophysical properties of the various complexes were investigated both in the solid state and in solution. At room temperature, luminescence was observed for the mononuclear salts $[CuL_4]PF_6$ for L = py, py-d_5, pic, or phpy as well as for $[Cu(lut)_3]PF_6$ but not for $[Cu(acn)_4]PF_6$ or $[Cu(lut)_2]PF_6$, nor for any of the complexes in room temperature solutions. At 77 K all of the $[CuL_4]PF_6$ salts were emissive, both as solids and in solutions in neat ligand or 4/1 EtOH/MeOH, as were solids of $[Cu(lut)_3]PF_6$ and $[Cu(lut)_2]PF_6$. As previously reported, $[Cu(bpy)_2]PF_6$ and $[Cu(phen)_2]PF_6$ are not emissive.[9f,10a] Emission spectra, lifetimes and excitation spectra are summarized in Table 2. Unless otherwise noted, all reported lifetimes were determined from emission decays that were well-fit to monoexponential functions.

Table 2. Emission Maxima,[a] Excitation Maxima,[a] and Emission Lifetimes[b] for CuL_x^+ Salts

	λ_{max}^{em} (nm)	λ_{max}^{ex} (nm)	τ_{em}[c] (μs)
$[Cu(py)_4]PF_6$ (**II**)			
solid 298 K	525	411	8.1
solid 77 K	555	405	14.1
in pyridine 77 K	578	350	15.2
$[Cu(py\text{-}d_5)_4]PF_6$ (**II**-d_5)			
solid 298 K	524	400	13.3
solid 77 K	550	400	23.2
$[Cu(phpy)_4]PF_6$ (**VI**)			
solid 298 K	580	461	1.1
solid 77 K	604	440	16.5
$[Cu(pic)_4]PF_6$ (**V**)			
solid 298 K	529	408	12.9
solid 77 K	584	396	25.7
in picoline 77 K	578	350	17.0
$[Cu(acn)_4]PF_6$ (**I**)			
solid 298 K	no emission		
solid 77 K	560		22.6
$[Cu(lut)_3]PF_6$ (**IV**)			
solid 298 K	460	360	16.5
solid 77 K	470	360	55.0
in lutidine 77 K	580	350	14.6
$[Cu(lut)_2]PF_6$ (**III**)			
solid 298 K	no emission		
solid 77 K	470	330	28.6
in lutidine 77 K	580	370	13.3

[a] Data collected on a SPEX Fluorolog II system. [b] Excitation with 355 nm YAG harmonic. Detection at λ_{max}^{em} with an RCA 8852 photomultiplier tube and Tektronix 5912 digitizer. Lifetimes computed with a curve fit routine in the ASYST package. [c] Lifetime uncertainty ±10%.

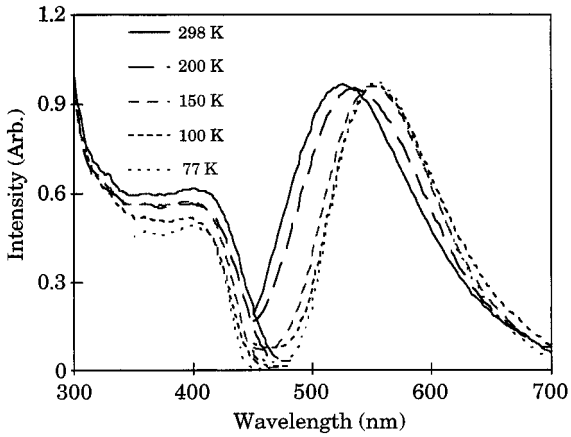

Figure 3. Emission and excitation spectra of solid $[Cu(py)_4]PF_6$ at different *T* (maximum emission intensities normalized to 1.0).

It is notable that the emission behaviors of the luminactive tetracoordinate complexes $[CuL_4]PF_6$ do not differ greatly from each other. For the solids at 77 K, the λ_{max}^{em} values range from 550 to 604 nm, and the range of τ^{em} values is 14−26 μs. Greater differences were found for those with other coordination symmetries; *i.e.*, the emission spectra of $[Cu(lut)_3]PF_6$ and $[Cu(lut)_2]PF_6$ both display λ_{max}^{em} at 470 nm but the 77K τ^{em} values are 55 and 28 μs, respectively.

Luminescence from solid $[Cu(py)_4]PF_6$ proved to be bright green at room temperature but orange at 77 K with the red shift in λ_{max}^{em} occurring systematically as *T* was lowered (Figure 3). The excitation spectrum displayed a small blue shift over the same temperatures. Notably, the color of the powdered salt

(34) Ford, P. C.; Rudd, De F. P.; Gaunder, R.; Taube, H. *J. Am. Chem. Soc*. **1968**, *90*, 1187.
(35) *Handbook Series in Organic Electrochemistry*; Meites, K., Zuman, P., Eds.; Chemical Rubber Co.: Cleveland, OH, 1976; Vol. 1.

changes from yellow at ambient T to white at 77 K, and one might speculate that the MLCT absorption band sharpens as the temperature is lowered and no longer tails into the visible. The first feature in the excitation spectrum is a $\lambda_{max}^{ex} \sim 400$ nm rising from a band edge onset about 450 nm, which parallels features of the diffuse reflectance spectrum (Figure 2). A plot of $\log(\nu_{max}^{em})$ versus T^{-1} for the emission maximum of solid **II** shows a discontinuity at ~200 K, suggesting a solid phase transition.

Quantum yields were determined for emission from the room temperature solids $[Cu(py)_4]PF_6$, $[Cu(py\text{-}d_5)_4]PF_6$, and $[Cu(lut)_3]PF_6$ by the method of Wrighton *et al.*[27] over the excitation wavelength range of 320−420 nm. These values proved to be surprisingly large: 0.22 for **II**, 0.38 for **IV**, and 0.29 for perdeuterio **II** $\lambda^{ex} = 375$ nm**.** There was considerable scatter (±25%) in the values determined for **IV** at various wavelengths, and the Φ^{em} values for **II** and perdeuterio **II** fell off systematically at the shorter λ^{ex} in a manner suspected to be artifactual owing to considerable absorption of the solid at these wavelengths. Nonetheless, at each excitation wavelength, the Φ^{em} from $[Cu(py\text{-}d_5)_4]PF_6$ proved systematically ~25% higher than for **II**, and **IV** was even more strongly emissive. The larger quantum yield for the perdeuterio complexes is paralleled by its similarly longer lifetime (Table 2) and can thus be attributed to deuteration-induced slowing of nonradiative deactivation as has been reported for other systems.[36]

Substituent effects may be helpful in establishing the orbital parentage of an absorption or emission band.[34,37] In this context, the emission spectra can be compared for tetrakis complexes of the 4-substituted pyridines py, pic, and phpy. Somewhat surprisingly, the emission bands for the 77 K solids of both $[Cu(pic)_4]PF_6$ and $[Cu(phpy)_4]PF_6$ are both red shifted (by 29 and 49 nm, respectively) from the λ_{max}^{em} of $[Cu(py)_4]PF_6$. At first glance this would not appear to be consistent with the relative energies expected for MLCT excited states, since the electron donating 4-methyl of picoline should raise ligand π^* orbitals energies (relative to analogous pyridine orbitals), but the greater delocalization of 4-phenylpyridine should lower the energies of the analogous orbitals. In that context, while the red shift of λ_{max}^{em} for **VI** would appear to support a MLCT assignment, the red shift for **V** would not. However, the substituents also affect the σ-donor abilities of these ligands, and stronger σ-donation to the metal center from the four L's would also serve to stabilize a MLCT state. The pK_a's of these ligands follow the order 4-picoline > 4-phenylpyridine ~ pyridine,[38] so picoline should be the stronger σ-donor. As a result, the response of the MLCT energy to substituent effects is difficult to predict.

For the solid $[CuL_4]PF_6$ salts, the high-energy tail of the emission band appears to overlap the low-energy tail of the lowest energy excitation band. Notably, for solid **II**, the first excitation band (Figure 3) is nearly the same as the lowest energy band in the diffuse reflectance spectrum (Figure 2). This suggests that the excitation band is a direct transition into the emitting state. From the overlap of such spectra, one can also estimate E^{00} energies of the emitting state. For $[Cu(py)_4]PF_6$ at 77K this is estimated to be 2.17 μm^{-1}, a value close to the average of ν_{max}^{ex} and ν_{max}^{em}, which is 2.14 μm^{-1}. Similar averaging of ν_{max}^{ex} and ν_{max}^{em} gives E^{00} estimates of 2.12 and 1.96 μm^{-1} for **V** and **VI**, respectively.

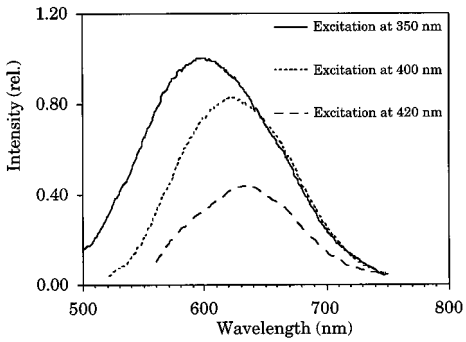

Figure 4. Emission from a 10 mM Cu^I solution of in 1/4 (v/v) piperidine/butylbenzene (77 K). (Intensities are normalized to the emission from 350 nm excitation.)

No emission was observed for ambient temperature solutions of any compound described in Table 2. Although the various copper(I) complexes partially dissociate when dissolved in 298 K 4/1 ethanol/methanol solution (see above), some emission was observed for such solutions at 77 K. The emission spectra and lifetimes of these solutions differ from the solids (hence argue against formation of microcrystalline precipitates) and are similar to the properties of the same salts dissolved in their neat ligands at 77 K. Nonetheless, given considerable uncertainty about the CuL_4^+ ions in EtOH/MeOH, these observations will not be described further. Emission spectra and lifetimes were also recorded for 77 K solutions of **II** in pyridine, **V** in picoline and **III**, and **IV** in lutidine (Table 2). As might be expected the properties of **III** and **IV** under these conditions were (within experimental uncertainty) identical, since the bis complex **III** forms the tris analogue in excess lutidine. In each case, the λ_{max}^{em} was found at longer wavelength than for the respective solids, the shifts being the largest for the lutidine complexes. Also λ_{max}^{ex} appeared at shorter wavelength in each case compared to the respective solid, presumably because the much lower effective concentrations of the solutions make absorption into the lowest energy spin forbidden bands less probable.

Emission was detected from $[Cu(acn)_4]PF_6$ in the solid state at 77 K using the fourth harmonic (266 nm) of the YAG laser as the excitation source. The band position ($\lambda_{max}^{em} = 590$ nm) and lifetime ($\tau^{em} = 22.6$ μs) proved to be similar to those observed for other $[CuL_4]PF_6$ salts. No emission was detected at room temperature.

Attempts were made to prepare homoleptic copper(I) complexes of the saturated amine piperidine (c-$C_5H_{10}NH$) from $[Cu(acn)_4]PF_6$ under Ar using Schlenk techniques in a manner analogous to the preparation of **II**. However, the 77 K emission properties of the solid products varied irreproducibly from batch to batch. More consistent spectroscopy was obtained by *in situ* studies of solutions prepared by dissolving $[Cu(acn)_4]PF_6$ (10−100 mM) in 4/1 (v/v) butylbenzene/piperidine (Figure 4). The UV/vis absorption spectra of these solutions displayed only a weak shoulder ($\epsilon \sim 200$ M^{-1} cm^{-1} at 350 nm) at $\lambda > 280$ nm. Emission spectra at 77 K showed λ_{max}^{em} in the range of 590−640 nm dependent on λ^{ex} (varied from 350 to 420 nm). For a single λ^{ex} (*e.g.*, 350 nm), λ_{max}^{em} did not depend on [Cu] (10−100 mM), but τ's, which fell in the range 4.6−9.6 μs, were dependent on both [Cu] and observation wavelength. It is likely that these properties reflect the behavior of a mixture of species, the bis- and tris(piperidine) complexes and perhaps the tetrakis complex.

Possible Assignments of Luminescence Bands. Qualitative assignment of the state or states responsible for the photophysical properties must account for several important observations. Both room temperature and 77 K emission lifetimes in most

(36) Frink, M. E.; Ford, P. C. *Inorg. Chem.* **1985**, *24*, 1033−1035, and references cited therein.
(37) Ford, P. C. *Rev. Chem. Intermed.* **1979**, *2*, 267−296.
(38) Schofield, K. *Hetero-Aromatic Nitrogen Compounds: Pyrroles and Pyridines*; Butterworths: London, 1967; p 146.

Table 3. Calculations on Copper(I) Ammines[a]

	Cu^+	$Cu(NH_3)^+$	$Cu(NH_3)_2^+$	$Cu(NH_3)_3^+$	$Cu(NH_3)_4^+$
LEES (Franck−Condon)	^3E (T_d)	^3A (C_1)	$^3A'$ (C_s)	$^3A'$ (C_s)	$^3B_1$ (T_d)
ΔE [b]	0.063	0.058	0.112	0.121	0.072
ΔCu 4p [c]	0.000	0.180	0.000	0.000	0.000
ΔCu 4s [c]	1.000	0.701	0.792	1.054	1.211
ΔCu 3d [c]	−1.000	−0.863	−0.696	−0.807	−0.743
ΔCu(tot.) [c]	0.000	0.017	0.096	0.247	0.467
ΔMOP(M−L)[d]	0	−0.025	−0.359	−0.485	−0.555

[a] Calculations of the cuprous amine complexes were based on the estimated Cu−N bond distance of 1.85 Å. [b] Calculated energy relative to GS. [c] Change in electronic population relative to GS. [d] Change in the Mulliken overlap population correponding to metal−ligand covalent bonding.

cases exceed 10 μs. This suggests that the transitions leading to luminescence are forbidden, most likely spin-forbidden triplet ES to singlet GS transitions. Furthermore, while the emissions from the tetrakis(aromatic amine) complexes such as $[Cu(py)_4]PF_6$ are the more intense and better behaved, bands with similar λ_{max}^{em} and τ^{em} values were seen at 77 K for the tetrakis(acetonitrile) complex **I** and for species formed in the reaction of **I** with excess piperidine, a saturated amine. The absence of aromatic π^* orbitals in these cases argues against general assignment of the emissions as being from low-lying MLCT excited states, and copper centered d → s states certainly come to mind as possibly significant players, at least for the latter species. In the context of these concerns, the *ab initio* calculations described in the next section were initiated.

Computational Studies. *Ab initio* studies of molecules with heavy atoms were possible with the COLUMBUS programs, which employ relativistic corrected core potentials. These calculations were at the restricted Hartree−Fock level, which can provide valuable insight into the characters of frontier orbitals and excited states prepared by electronic excitation between these. The RHF-SCF calculation usually converges to the lowest state of a given multiplicity and symmetry, but such ES are of particular interest here since they are the most likely to be involved in luminescence. The ES calculations used GS structural parameters and did not optimize ES structures, nor did they take configuration interaction into account. Thus, the calculations provide qualitative insight regarding the orbitals and energies of GS and Franck−Condon states but are less reliable from the quantitative perspective. In several cases, calculations were repeated with a systematically varied structural parameter, *e.g.*, the metal ligand bond length, to probe qualitative energy/structure relationships for selected states. Notably, the order of calculated ES energies often does not parallel that of ΔE's between the orbitals involved in the electronic excitation, since self-compensating electronic relaxation accompanys.[20] Thus, the ES generated from the HOMO−LUMO transition is not always the lowest energy excited state (LEES), and electronic distributions of computed ES may differ significantly from those suggested by GS orbital parentages.

Such calculations were carried out for ground and excited states of the real and hypothetical complexes $Cu(NH_3)_n^+$ and $Cu(py)_n^+$ ($n = 1-4$) plus $Cu(acn)_4^+$. The spectroscopic data suggest that the most likely assignments of the emitting ES for these cuprous complexes are parity forbidden, metal localized d → s,p states. These *ab initio* calculations were initiated to probe the validity of this conclusion. Since the emphasis is on the spectroscopy, results of the calculations will be largely presented in terms of differences between GS and ES electronic distributions as the result of electronic excitation. The GS calculations for these and related complexes are described in more detail elsewhere.[1]

(a) Cu^+ and $Cu(NH_3)_n^+$. The bare Cu^+ ion, which could only be calculated under lower symmetries,[29] was also considered. The groups T_d, D_2, and C_1 were all used with no substantive differences in the results. Under T_d symmetry, the Cu^+ ground state has an energy of −49.9493 hartrees (1 hartree = 219 475 cm^{-1}) and the five d orbitals were energetically degenerate. The calculated energy gap between the highest occupied orbital (HOMO), a Cu 3d, and the lowest unoccupied orbital (LUMO), the Cu 4s, is 0.553 hartree. The LEES proved to be the result of a d → s transition, but the calculated ES energy (0.063 hartree) was much less than the orbital energy difference owing to reduced electron repulsion on going from a $(3d)^{10}$ to a $(3d)^9(4s)^1$ configuration in addition to the usual shortcoming of virtual orbital energies in Hartree−Fock theory. Comparison of these results with experimental spectroscopic data[39] shows a reasonable correspondence, although the computed lowest energy d → s transition energy is about 85% that determined from spectroscopy, and the calculated singlet−triplet energy difference was 0.013 hartree vs 0.020 hartree in the experiments.

Calculations for the cuprous ammines $Cu(NH_3)_n^+$ ($n = 1-4$) showed that all of the complexes display a HOMO−LUMO energy gap less than that of the cuprous ion alone (0.043 hartree for $n = 4$), owing to the antibonding 3d orbitals being raised in energy by interactions with ligands. The net charge of the metal decreased somewhat due to GS charge transfer from the ammines. Net covalent metal−ligand bonding in the complexes, as defined as the sum of the Mulliken overlap populations (MOP(M−L)),[20] were small and appeared to be largely due to stabilization of occupied 3d orbitals by increased mixing with the 4s and 4p orbitals. The bonding in such complexes must be largely due to charge−dipole interactions.

The LEES of each $Cu(NH_3)_n^+$ ion was found to be the result of the HOMO → LUMO transition, the energy of which was again found to be much smaller than the orbital energy gap. As shown in Table 3, this LEES is predominantly d → s in character, although there is significant charge transfer to the metal in the LEES of the tri- and tetraammine complexes. Correspondingly there is a greater decrease in the metal−ligand covalent bond order (ΔMOP(M−L)) in going from the GS to the LEES for larger values of *n*. Higher energy states explored were predominantly copper 3d → 4p and LMCT in character, with the lowest Cu "3d → 4p" state ∼0.03 hartrees and the lowest LMCT state ∼0.2 hartrees higher in energy than the LEES.

The increased electron density at the copper can be largely attributed to electronic reorganization lending LMCT character to the LEES. The trend can be rationalized in terms of electronic reorganization as follows. The HOMO−LUMO transition is largely d−s in orbital parentage, but, upon excitation, the d orbital energy drops due to decreased electron−

(39) *Atomic Energy Levels*; Moore, C., Ed.; National Bureau of Standards: Washington, D.C., 1949; Vol. II.
(40) Baglio, A.; Weakliem, H. A.; Demelio, F.; Vaughn, P. A. *J. Inorg. Nuc. Chem.* **1970**, *32*, 795−801.
(41) Csoregh, I.; Kierkegaard, P.; Norrestam, R. *Acta Crystallogr.* **1975**, *B31*, 314−317.

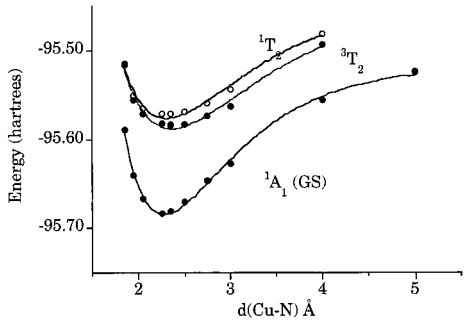

Figure 5. $Cu(NH_3)_4^+$ potential surfaces weighted fit to a Morse potential.

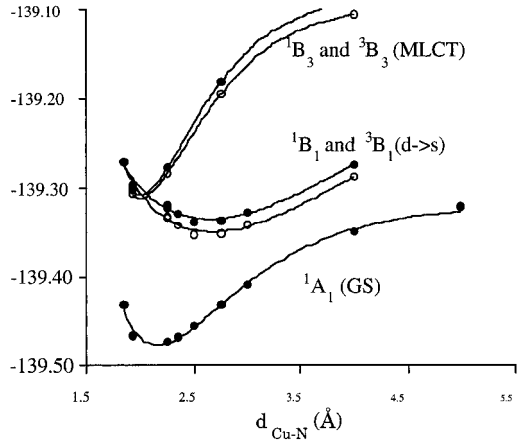

Figure 6. $Cu(acn)_4^+$ potential surfaces weighted fit to a Morse potential.

Table 4. $Cu(acn)_4^+$ Excited State Calculations (Double ζ Basis Set; D_2 Symmetry)[a]

state	ΔE [b] (hartree)	ΔCu 4s [c]	ΔCu 4p [c]	ΔCu 3d [c]	ΔCu (tot.) [c]	ΔMOP(M−L) [d]
$^3B_3$	0.159	0.062	0.393	−0.786	−0.331	0.020
$^3B_1$	0.164	0.900	0.050	−0.796	0.156	−0.497
$^3A_1$	0.179	0.905	0.056	−0.827	0.135	−0.503

[a] Structure used for $Cu(acn)_4^+$ calculations was the published structure with Cu−N = 1.99 Å.[41] [b] Calculated energy relative to GS. [c] Change in electronic population relative to GS. [d] Change in the Mulliken overlap population correponding to metal ligand covalent bonding.

electron repulsion terms. The consequential electronic reorganization involves a flow of charge from ligand localized orbitals into metal localized or metal−ligand antibonding orbitals. This is more pronounced with a higher *n* where the coordination sphere is electron rich. The larger net effect decreases metal−ligand bonding, as shown by the ΔMOP(M−L) values, thus generates greater distortions between ground and excited states.

One dimensional energy surfaces can be generated by repeating the calculations for a series of different fixed M−L distances. Figure 5 illustrates such surfaces calculated for $Cu(NH_3)_4^+$ under T_d symmetry and fit to a Morse potential for the ground ($^1A_1$) and the two lowest excited states ($^3T_2$ and $^1T_2$). Each of these is bound, although the ES are more weakly bound than the GS (D_e = 0.166 hartree for $^1A_1$, 0.138 hartree for $^3T_2$, and 0.129 hartree for $^1T_2$). The ES minima are distorted from the calculated Cu−N bond length (2.274 Å) of the GS minimum by 0.091 Å for the $^3T_2$ state and 0.039 Å for $^1T_2$. For comparison, the Cu−N bond lengths for the cupric salt $[Cu(NH_3)_4][CuI_2]_2$ were determined by crystallography to be 2.114−2.163 Å.[42] Such M−L bond lengthening at the d → s ES minimum is consistent with the negative ΔMOP(M−L) values computed for the Franck−Condon state (Table 3).

(b) $Cu(CH_3CN)_4^+$. Calculations on the tetrakis(acetonitrile) complex **I** were based on bond length data taken from the crystal structure.[41] It was not possible to obtain satisfactorily converged ES wave functions under T_d symmetry. For this reason, D_2 symmetry was imposed on the molecule, and the results of double ζ basis set calculations are summarized in Table 4. The results of these calculations show several triplet Franck−Condon states with different orbital parentages to have very similar energies. The lowest energy $^3B_3$ state involves significant charge transfer from the metal and is predominately MLCT in character. The $^3B_1$ state, which is marginally at higher energy, is predominately d → s in character with a modest (15%) contribution of LMCT in the manner seen with ammine complexes. The sums of the Mulliken overlap population of the Cu−N bonds change as well, with a small positive ΔMOP(M−L) value accompanying the Franck−Condon transition from GS to $^3B_3$(MLCT), but a very substantial decrease accompanying the Franck−Condon transition from GS to $^3B_1$(d→s) (Table 4).

The situation changes when nuclear relaxation is considered. Although calculations did not allow a practical consideration of all nuclear coordinates, it was possible to examine the energies of the GS, the $^3B_3$(MLCT) state, and the $^3B_1$(d→s) state as a function of systematically varied M−L bond distances. These calculations are summarized in Figure 6, where the one-dimensional potential energy surfaces are Morse type curves fit to the computational results. In this manner, the minimum for the GS gave a Cu−N distance of 2.165 Å, about 8% larger than the value of 2.000 Å determined by X-ray crystallography,[41] and the minima for the $^3B_3$(MLCT) and $^3B_1$(d→s) states gave Cu−N distances of 2.018 and 2.631 Å, respectively. Thus, the directions of the predicted distortions from initially formed Franck−Condon states to the minima of the one-dimensional potential energy surfaces are consistent with computed changes in Mulliken overlap populations. Furthermore, these computations indicated that relaxation along these one-dimensional surfaces could even reverse the excited state order. The minimum of the $^3B_1$(d→s) (0.124 hartree above the GS minimum) is now substantially lower energy than that of the $^3B_3$(MLCT) surface (0.169 hartree). The analogous singlet state minima are 0.013 and 0.003 hartree above those of the respective triplets. Thus, once this aspect of nuclear relaxation is taken into account, the lowest energy excited state is clearly the $^3B_1$(d→s) and is the likely ES responsible for the luminescence of **I**.

One-dimensional potential surfaces for the ground and $^3B_1$(d→s) states of **I** were also generated by flattening the structure along the *z*-axis of the D_2 symmetry from nearly tetrahedral to square planar. This was done by opening the N−Cu−N angles bisected by the *z*-axis but holding the Cu−N distance fixed at that of the X-ray crystallography structure. The GS minimum occurred with these N−Cu−N angles at 104.9°, *i.e.*, close to the tetrahedral structure, and the maximum at 180°, *i.e.*, the square planar structure. The $^3B_1$(d→s) minimum was found at 180°, where these two surfaces come closer together but do not cross, the calculated energy difference decreasing from 0.167 to 0.122 hartree. Thus, these calculations clearly indicate that the metal−ligand bonds of the $^3B_1$(d→s) ES should undergo both radial and angular distortion from the GS geometry.

(c) $Cu(py)_n^+$. When calculations were carried out for the $Cu(py)_n^+$ series (n = 1−4), the natures of the HOMO and

(42) Parke, S.; Webb, R. S. *Phys. Chem. Glasses* **1972**, *13*, 157−160.

Table 5. Excited State Calculations for $Cu(py)_n^+$ [a]

	$Cu(py)^+$	$Cu(py)_2^+$		$Cu(py)_3^+$		$Cu(py)_4^+$
LEES	$^3A_1$ (C_{2v})	$^3A_1$ (C_{2v})	$^3B_1$ (C_{2v})	$^3B_1$ (C_{2v})	$^3B_1$ (C_{2v})	$^3B_1$ (D_2)
ΔE [b] (hartree)	0.043	0.104	0.162	0.114	0.116	0.091
ΔCu 4p [c]	0.162	0.043	0.160	0.049	0.186	0.233
ΔCu 4s [c]	0.809	0.888	−0.091	1.276	0.118	0.195
ΔCu 3d [c]	−0.919	−0.730	−0.722	−0.828	−0.790	−0.785
ΔCu(tot.) [c]	0.052	0.203	−0.650	0.495	−0.487	+0.357
ΔMOP(M−L)[d]	0.010	−0.335	0.107	−0.386	0.163	0.037

[a] Structures used for $Cu(py)_n^+$ calculations were as follows. For $Cu(py)^+$ the structure was assumed to be analogous to the unique ligand of the $Cu(lut)_3^+$ structure with Cu−N = 2.046 Å.[25] For $Cy(py)_2^+$, the structure was assumed analogous to that of the $Cu(lut)_2^+$ ion with Cu−N = 1.85 Å.[24] For $Cu(py)_3^+$ the structure was assumed analogous to that of $Cu(lut)_3^+$ with one Cu−N at 2.046 Å and two at 2.00 Å.[25] That used for the $Cu(py)_4^+$ calculations was the published structure with Cu−N = 2.046 Å.[22] [b] Calculated energy relative to GS. [c] Change in electronic population relative to GS. [d] Change in the Mulliken overlap population correponding to metal−ligand covalent bonding.

LUMO were found to depend on the value of *n*. For $n = 1$, a ligand π-orbital proved to be the HOMO and the nearest Cu 3d orbital was found to be 0.087 hartree lower in energy. The LUMO was the Cu 4s. For $n = 2$, the HOMO is again a ligand π-orbital, but now the highest energy copper 3d orbital is but 0.035 hartree below it. Furthermore, as seen with the cuprous ammines, increasing the coordination number also raises the energies of the 4s and p orbitals so that the LUMO is now a π_L*-orbital. For $n = 3$, the gap between the highest energy Cu 3d and the ligand π-orbital HOMO is even smaller (0.015 hartree), while for $n = 4$, the HOMO is principally of Cu 3d character and is 0.013 hartree above the highest π_L-orbital. In both cases the LUMO is a ligand π_L*-orbital.

Ab initio calculations were carried out for the ground state and for excited states formed by the lower energy orbital transitions for $n = 1-4$ (Table 5). For the mono-pyridine copper complex, the LEES is of $^3A_1$ symmetry principally 3d → 4s in character and an energy 0.043 hartree above the GS. The $^3A_2$ LMCT state formed from the HOMO (π_L) to LUMO (Cu 4s) transition was found at significantly higher energy (0.189 hartree) as were the $^3B_2$ ligand localized $\pi\pi$* state formed from the HOMO to lowest energy π_L* transition (0.177 hartree) and the $^3B_1$ MLCT state formed by the transition from the highest energy 3d orbital to the lowest energy π_L* (0.248 hartree).

The LEES of the bis(pyridine)copper(I) complex is also a $^3A_1$(d→s) state (0.104 hartree). The HOMO−LUMO transition gives a $^3B_2$ $\pi_L\pi_L$* state which has much higher energy (0.261 hartree). The calculations showed a $^3B_1$ MLCT state at an intermediate energy (0.162 hartree) (Table 5) but were unable to compute the $^3A_1$ MLCT state (from the transition from the highest energy 3d orbital to the lowest energy π_L*-orbital) which would be expected to appear at a slightly lower energy. The calculations converged to the lower energy $^3A_1$(d→s) state instead. The energy difference between the two lowest π_L* acceptor orbitals is but 0.01 hartree, so the $^3A_1$ MLCT state should be significantly higher energy than the $^3A_1$(d→s) state.

For the tris(pyridine)copper(I) ion, there was little difference in the energies computed for the lowest (d → s) and MLCT Franck−Condon excited states. The LEES is the $^3B_1$(d→s) with considerable LMCT character, but the $^3B_1$ MLCT state, from a 3d to the π_L* LUMO transition is only negligibly higher in energy (Table 5). The HOMO to LUMO transition, between a π-orbital delocalized over two pyridines to a π_L*-orbital on the third, gave a $^3A_2$ ligand to ligand charge transfer (LLCT) state of much higher energy (0.262 hartree).

Calculations of lower energy excited states for the $Cu(py)_4^+$ ion converged to the $^3B_1$ and $^1B_1$ MLCT states formed from the HOMO → LUMO transition (0.091 hartree). The energies of these were lower than for any of the respective triplet and singlet MLCT states computed for the other members of the $Cu(Py)_x^+$ series. Attempts were specifically made to compute the lowest energy singlet and triplet d → s states of $Cu(py)_4^+$ by starting the calculations with wave functions appropriate for the HOMO → 4s orbital transition. However, the SCF iterations converged to the computationally lower energy $^3B_1$ and $^1B_1$ MLCT states of the same symmetries.

The mono-, bis-, and tris(pyridine)copper complexes for which Cu d → s states could be calculated displayed the same trend as the copper ammine series with regard to increasing LMCT character of the ES as the coordination number *n* increased (Tables 3 and 5). In the same context, these ES displayed substantially negative ΔMOP(M−L), values indicating the tendency of these states to undergo distortion to longer Cu−N bonds. In contrast, metal−ligand bonding appears to be enhanced in the MLCT states. The presence of relatively low-lying MLCT states for those complexes of higher coordination number is the result of the raised energy of the metal 3d orbitals as the coordination sphere becomes more electron rich. MLCT bands are observed in the absorption spectra of these complexes and tend to shift to lower energies as *n* increases.

Comparisons of Spectroscopic and Theoretical Results

The common theme of the above calculations is that a metal centered, d → s ES is either the lowest energy Franck−Condon state or close in energy to this state. The tetracoordinated complexes $Cu(acn)_4^+$ and $Cu(py)_4^+$ are exceptions to this qualitative conclusion, although allowing the former to relax along Cu−N coordinates clearly reversed the ES order, so that the d → s was concluded to be the LEES. Thus, for the poorly characterized Cu(I) piperidine complexes, for the two lutidine complexes **III** and **IV** and for the acetonitrile complex **I**, the assignment of the emitting excited state as the d → s ES appears appropriate. As noted calculations with the tetrakis(pyridine) complex **II** were not successful in estimating the energies of any ES except the lowest energy MLCT Franck−Condon state, so it was not resolved whether extending the copper ligand bond lengths would bring the d → s ES into the appropriate energy range in this case. One is tempted to elect a MLCT assignment for the emission bands from **II** given the observation of modest substituent effects for the 4-picoline and 4-phenylpyridine CuL_4^+ analogues. Both the *p*-methyl and *p*-phenyl substituents shift the band to lower energy, but this may be explained in terms of the greater basicity of both ligands (relative to py) and the theoretical demonstration that electron donation at the coordination site lowers the energy of MLCT states. Nonetheless, a d → s orbital parentage of the luminactive state of **II** would be consistent with the similarities of respective emission band positions, shapes, and lifetimes for solids **I** and **II**.

The lowest excited states of the diimine complexes such as $[Cu(bpy)_2]PF_6$ and $[Cu(phen)_2]PF_6$ should be MLCT in character

owing to the much lower energies of the delocalized π_L*-orbitals. However, the diimine complexes are not luminescent unless the coordination environment is made bulkier by groups in ortho positions such as in the luminactive salts of $Cu(dmp)_2^+$ and $Cu(dpp)_2^+$. A rationalization for such behavior is that the steric bulk reduces the tendency of the MLCT states, which formally have a d^9 Cu(II) center, to undergo a Jahn−Teller distortion which would decrease the energy gap between the LEES and GS and accelerate nonradiative deactivation.[9f] Such a mechanism would be expected to play a role in deactivating MLCT states of $Cu(py)_4^+$ and its analogues, since these should also be relatively free to distort. Flattening of the tetrahedral complex was also predicted for a d → s state, but a substantial energy gap remained. Such arguments support the view that the LEES of **II** is predominantly d → s rather than MLCT in character.

Analogy can be drawn between photophysical properties of the complexes in the present study and those displayed by cuprous ions doped into phosphate, silicate, and borate glasses at low loadings (1.25%).[42] Those glasses displayed absorptions at ∼250 nm, assigned as the allowed 3d → 4p transitions. Excitation at this wavelength produced emissions with maxima in the 450−600 nm range, depending on the glass and 298 K lifetimes ranging from 26 to 33 μs. The large Stokes shifts, emission wavelength range and microsecond lifetimes are features shared by the luminescence properties of the discrete copper(I) coordination complexes described here.

Comparison should also be made the luminactive behavior of the tetrameric cluster $Cu_4I_4(py)_4$ (**A**) which displays a broad emission at $\lambda_{max} = 580$ nm with a λ^{em} of 11 μs from the 298 K solid.[3d] This is somewhat lower energy than the 298 K solid state emission bands of the mononuclear complexes summarized in Table 2, and the difference is even more pronounced for spectra obtained in solutions. This emission has been assigned on the basis *ab initio* calculations[20] as being from a "cluster centered" excited state of **A** having roughly equal contributions of "3d to 4s" and iodide "p" to copper "s" charge transfer character, in both cases the metal "s" being a σ^b orbital delocalized over the four metal centers. The Cu d → s state of $Cu(py)_4^+$ could not be computed, but extrapolation of the trend observed for the $Cu(py)_n$ species of lesser *n* (Table 5) suggest that such a state should also have a significant LMCT component. The lower energy of the tetramer CC* state relative to the monomer luminactive states may be the result of the delocalized nature of the s acceptor orbital as well as the higher energy of iodide (*vs* pyridine) orbitals. In both the mononuclear and cluster excited states, electron density in metal−ligand antibonding orbitals increases relative to the GS with a corresponding decrease in the Mulliken overlap populations of M−L bonds. However, the tetramer is different since the same orbitals are bonding with respect to metal−metal interactions so that the ES distortion occurs over several coordinates.

In summary, it is useful to recognize that a study combining spectroscopic and computational approaches can provide better insight into the nature of the excited states of these complexes than either method alone. Calculations on the excited states are necessary because conclusions based solely on the energies of ground state highest occupied and lowest unoccupied orbitals can be erroneous given that electronic reorganization upon excitation sometimes reverses the orders of relevant states. Complete GS and ES geometry optimization for these CuL_x^+ systems would be very attractive, but efficient computations of such are outside the capability of the current program. Calculated variations in overlap populations indicate the types of ES distortions that might be expected, but the information obtained by systematically varying selected geometrical parameters provides more quantitative insight into the relative responses of ES energies to distortions.

Acknowledgment. This research was supported by the U. S. National Science Foundation (Grants No. CHE-9024845, CHE 9400919). Laser flash photolysis experiments were carried out on a time resolved optical system constructed in part from support from a U. S. Department of Energy University Research Instrumentation Grant (No. DE-FG05-91ER79039) and in part from an NSF Instrumentation Grant. We thank Marcello Vitale for his assistance with the *ab initio* calculations and R. M. Pitzer of The Ohio State University for providing the COLUMBUS programs.

IC960367Y